Electrochemical Processes in a Wire-in-a-Capillary Bulk-Loaded, Nano-Electrospray Emitter

Gary J. Van Berkel, Keiji G. Asano, and Paul D. Schnier*

Organic and Biological Mass Spectrometry Group, Chemical and Analytical Sciences Division, Oak Ridge National Laboratory, Oak Ridge, Tennessee, USA

Experiments are described that illustrate solvent oxidation, emitter electrode corrosion, and analyte oxidation in positive ion mode nano-electrospray mass spectrometry using a wire-in-a-capillary, bulk-loaded nano-electrospray emitter geometry. Time-lapsed color photography of pH and metal specific indicator solutions within operating nano-electrospray emitters, as well as temporal changes in the ions observed in the nano-electrospray mass spectra, are used to probe these reactions, judge their magnitude, and study the time dependent changes in solution composition and gas-phase ion signal brought about as a result of these electrochemical reactions. The significance of these observations for analytical applications of nano-electrospray mass spectrometry are discussed. (J Am Soc Spectrom 2001, 853–862) Published by Elsevier Science Inc.

Nano-electrospray mass spectrometry (nano-ES-MS) generally refers to any ES-MS system that uses an emitter arrangement capable of operating at solution flow rates of about ten to a few hundred nanoliters/min [1]. This can be either a Wilm and Mann type bulk-loaded, spray capillary [2, 3] or any one of a variety of continuous flow-through devices that might be used for continuous infusion, flow injection, or as an interface for on-line CE/ES-MS or HPLC/ES-MS (e.g., [4–7]). The nano-ES ion sources possess most of the capabilities of the traditional ES emitters that operate at flow rates from the low microliter/min range to an upper limit of about one milliliter/min. An advantage of operating in the nanoliter/min flow rate regime is that a few microliters of a sample solution provide a continuous signal for 30 min or longer. This is very useful in the analysis of limited volumes of precious samples and also for tandem mass spectrometry (MS/MS) and MS^n experiments, which may take a considerable amount of time to optimize or complete [1–3]. Furthermore, sensitivity gains are made with such low flow rate devices and solutions difficult to spray with conventional ES spray emitters, such as 100% aqueous solutions, are more easily accommodated [1–7].

The first and still exploited approach to nano-ES-MS follows the design of Mann and Wilm [2, 3]. A glass capillary with a spray tip pulled to a narrow external and internal (<20 μm) diameter [1–3] is loaded with one or more microliters of sample solution. A modest gas pressure (several psi) may be applied to help maintain a steady solvent flow. The necessary high electric field between the bulk-loaded solution to be sprayed from the emitter and the counter electrode in the ion source (normally the entrance aperture plate or inlet capillary of the mass spectrometer) is achieved by one of two basic methods. The first method makes electrical contact to the solution (either high voltage or ground depending on the particular interface) via a metal [1–3] or other conductive coating [8] that is on the exterior of the capillary tip. The liquid exiting the capillary touches the electrical contact only at the edges of the narrow tip. This electrode geometry might be viewed as a very short tubular electrode [9]. Emitters of this geometry do not have a particularly long, useful lifetime, due mainly to poor mechanical or electrochemical stability of the conductive contact [10, 11]. The second method of making electrical contact to solution is to simply immerse a metal wire in the solution within the capillary [12, 13]. In our hands, this electrode arrangement proves more robust and reliable than the other, and, in contrast to another report [13], requires no particular care in positioning the wire other than to terminate it near the spray tip end of the capillary.

Given the lack of any debate in the literature, whether one or the other of these two electrode configurations is used, apparently has little effect on the successful nano-ES-MS analysis of the most common types of analytes (e.g., peptides, proteins and oligonucleotides). However, the electrode geometrical arrangement and the electrode composition is expected to influence the electrochemical reactions that must occur

Published online May 14, 2001

Address reprint requests to Dr. G. J. Van Berkel, Chemical and Analytical Science Division, Oak Ridge National Laboratory, P.O. Box 2008, Oak Ridge, TN 37831-6365. E-mail: vanberkelgj@ornl.gov

* Present address: Pro-Neuron, Inc., 16020 Industrial Drive, Gaithersburg, MD 20877. E-mail: PSchnier@pro-neuron.com

Published by Elsevier Science Inc.
1044-0305/01/$20.00
PII S1044-0305(01)00264-1

Received December 4, 2000
Revised March 1, 2001
Accepted March 8, 2001

at the electrode for a continuously stable ES to be generated. The electrical contact to solution at the ES emitter is the working electrode in a controlled-current electrochemical flow cell [14–16]. In positive ion mode, oxidation reactions at this electrode supply the excess positive charge required to maintain the production of positively charged ES droplets. In negative ion mode, reduction reactions are responsible for maintaining the required supply of excess negative charge to produce negatively charged droplets. At a minimum, the size and shape of the electrode contact to solution, and the solution flow rate through/over the electrode will affect the current density and the mass transport to the electrode. Each of these factors will in turn influence the interfacial potentials at the electrode and the nature and extent of various electrochemical reactions that occur [9].

In this paper, we present experimental results that represent the major categories of electrochemical reactions in positive ion mode nano-ES-MS that might be expected with the wire-in-a-capillary, bulk-loaded nano-ES emitter geometry, viz., solvent oxidation, electrode corrosion, and analyte oxidation. Time-lapsed color photography of pH and metal-specific indicator solutions within operating nano-ES emitters, and temporal changes in the ions observed in the nano-ES mass spectra, illustrate the general phenomenology, magnitude, and time dependence of the changes in solution composition and gas-phase ion signal brought about as a result of the electrochemical reactions. The significance of these observations in practical applications of nano-ES-MS using the wire-in-a-capillary design are discussed.

Experimental

Chemicals

Sample solutions were prepared using deionized H_2O (Milli-RO 12 Plus, Millipore, Bedford, MA), CH_3OH (HPLC grade, J. T. Baker, Phillipsburg, NJ), CH_3CN (Baker), CH_2Cl_2 (Baker), ammonium acetate (NH_4OAc 99.999%, Aldrich), acetic acid (HOAc, PPB/Teflon grade, Aldrich), and HNO_3 (Ultrex II grade, Baker). All pH indicators were purchased from Aldrich and prepared at the concentrations recommended by Green [17] in H_2O containing 10–20% by volume CH_3OH. Approximately 100 μM KNO_3 was added to each indicator solution as an electrolyte to stabilize the spray and the ES current. The particular indicators and the literature reported pH color transitions were as follows: Congo red, pH 3.0 (blue) to pH 5.2 (red); quinaldine red, pH 1.4 (colorless) to pH 3.2 (red); chlorophenol red, pH 4.8 (yellow) to pH 6.4 (red); bromocresol green, pH 3.8 (yellow) to pH 5.4 (blue-green), methyl yellow, pH 2.9 (red) to pH 4.0 (yellow); and thymol blue, pH 1.2 (red) to pH 2.8 (yellow) [17]. An 8.4 μM nickel octaethylporphyrin (97%, Aldrich) solution was prepared in CH_2Cl_2/CH_3CN (1/1 v/v) containing 1.0 mM lithium trifluoromethanesulfonate (lithium triflate, 96%, Aldrich) as an electrolyte. A 1.0 mM solution of 1,10-phenanthroline (phen, Aldrich) was prepared in CH_3CN and stored in a plastic container prior to use.

Mass Spectrometry

All mass spectral data were acquired using a PE SCIEX API165 single quadrupole mass spectrometer (MDS SCIEX, Concord, Ontario, Canada) equipped with a nano-ES ion source (Protana A/S, Odense, Denmark). Glass nano-ES capillaries (normal tips, Protana A/S) approximately 5 cm long with a body o.d. of 1.2 mm and an i.d. of 0.69 mm were loaded with several microliters of sample solution. Electrical contact to solution was made by a platinum, stainless steel, iron, or copper wire (size and composition noted below) inserted into the liquid up to a point near the capillary spray tip. Applied voltages of 750–1000 V were required to initiate and sustain a stable spray.

Off-Line Optical Monitoring of the Nano-ES Emitters

Nano-ES emitters for off-line optical monitoring were constructed from 1.0 or 1.5 mm-o.d., 0.5 mm-i.d. borosilicate glass capillaries, which were pulled to about 5 μm-i.d. on one end using a micropipette puller (Sutter Instruments, Inc., Novato, CA). Electrical contact to solution was made by a wire inserted into the liquid as described above. Approximately 900 V was required to provide a stable flow and ES current (ca. 0.5 μA in all cases) with a grounded planar counter electrode placed 0.5 cm from the spray tip. ES currents were measured by grounding the counter electrode through a Keithley Model 610C electrometer (Cleveland, OH). Wires of four different compositions were used, viz., platinum (127 μm diameter, 99.99%, Aldrich, Milwaukee, WI), 304 stainless steel (250 μm diameter, Scientific Instrument Services [SIS], Ringoes, NJ), copper (250 μm diameter, 99.95%, SIS), and iron. The latter wire of unknown purity was salvaged from a J-type thermocouple (iron-constantan). Under normal operating conditions, solution flow rates were 10–100 nL/min. Time-lapse photographs were obtained with a color CCD camera (Panasonic Inc. Seacaucus, NJ) equipped with a telephoto lens. Color images (24-bit) were captured digitally using the Snappy video digitizer (Play, Inc., Rancho Cordova, CA) in 800 $\times$ 600 pixel format. For simplicity, the color scale for the pH indicators was constructed by photographing indicator solutions within the capillary which were titrated to pH values on either side of that indicator color transition. A linear interpolation of the color transition from the acid to the base form of the respective indicators produced the color scales shown in the figures. The color scale for the $[Fe(phen)_3]^{2+}$ complex was generated from photos of a 1.0 mM phenanthroline solution in the capillary with and without 50 μM Fe(II) (as $FeSO_4 \cdot 7H_2O$ in H_2O, Aldrich) added.

Results and Discussion

Solvent Oxidation

In positive ion mode, when using an electrical contact to solution that is electrochemically inert (e.g., platinum), oxidation of one or more of the major components of the solvent system will likely occur [18]. In an aqueous solvent, oxidation of H_2O (eq 1) might be expected to supply much, if not all, of the ES current.

$$O_2 + 4H^+ + 4e^- = 2H_2O,\ E^o = 1.229\text{V vs SHE [19]} \quad (1)$$

The occurrence of this reaction is equivalent to adding strong acid to the solution. Assuming this is the only reaction that takes place, the concentration of protons electrochemically added to solution can be calculated from Faraday's law as expressed in eq 2

$$[H^+]_{\text{elec}} = i_{ES}/(nFv_f) \quad (2)$$

where i_{ES} is the ES current, n is the molar equivalent of electrons involved in the production of one mole of H^+ (in this case $n = 1$), F is the Faraday constant (9.648×10^4 C/mol), and v_f is the volumetric flow rate out of the ES emitter. Assuming no buffering capacity in the solution and all product mixes completely and flows from the emitter as produced, the new or final pH of the bulk solution can be calculated from eq 3

$$\text{pH}_{\text{final}} = -\log([H^+]_{\text{elec}} + [H^+]_{\text{initial}}) \quad (3)$$

where $[H^+]_{\text{initial}} = 10^{-\text{pH}_{\text{initial}}}$.

As eqs 2 and 3 show, the magnitude of the pH change caused by H_2O oxidation is directly related to i_{ES} and inversely related to v_f. Because the magnitude of i_{ES} is only weakly dependent on solvent flow rate [20], and because published values for nano-ES currents [2, 3], as well as those we recorded here, are similar to conventional ES currents, the magnitude of any electrochemically induced pH change will increase as flow rate is decreased. We have previously shown that a bulk solution pH change of as much as 4 pH units ($\text{pH}_{\text{initial}} = 7.0$, unbuffered solution) might occur in ES assuming typical values of i_{ES} (i.e., 0.1 μA) and flow rates down to 100 nL/min [18]. In our nano-ES experiments, a typical value of i_{ES} was 0.5 μA and flow rates reached as low as 25 nL/min. Under these conditions, in an unbuffered solution of $\text{pH}_{\text{initial}} = 7.0$, a change of 5.1 pH units is calculated, resulting in a $\text{pH}_{\text{final}} = 1.9$. However, in the bulk loaded, wire-in-a-capillary nano-ES emitter, the situation is more complicated than this simple calculation would imply.

Figure 1a shows time lapse photographs of a pulled-glass capillary, nano-ES emitter tip that contains an H_2O/CH_3OH solution of the pH indicator congo red (pH $\leq$3.0, blue; pH $\geq$5.2, red). The high voltage contact to the solution is made via a platinum wire electrode placed to within about two millimeters from the capillary spray tip. The red color of the indicator in the capillary at the beginning of the experiment (0 min) is consistent with the measured initial solution pH of 5.8. After spraying continuously for 70 min, a color change to blue is observed from the wire tip out to the spray tip. At this point, the solution exiting the capillary in the spray must have a pH $\leq$3. The relatively long time period needed to observe a color change indicates that either the solution has a pH buffer capacity (contributed to by the indicator dye) or that the current efficiency for water oxidation is less than 100%. With an additional 20 min of spraying time (90 min), the blue form of the indicator is observed not only at the spray end, but also toward the back of the nano-ES capillary. In a pumped electrospray device, the electrochemical products (in this case protons) are swept from the capillary out into the spray. The bulk solution back from the spray tip is unaltered. This should also be true in the metal-coated glass capillary, bulk-loaded nano-ES emitter. As the present data demonstrate, however, in the wire-in-a-capillary nano-ES device, the whole sample volume can be altered by the electrochemical reactions, even if those reactions occur predominantly at the tip of the wire. This might be because upstream diffusion (or another mass transport phenomenon) of the products formed at the wire tip effectively competes with convective transfer (and possibly migration) of these products towards the spray tip. In any case, this observation suggests that the magnitude of alteration in solution composition caused by the electrochemical reactions cannot be simply calculated from the ES current and solution flow rate using Faraday's law.

The pH indicator used in the experiment shown in Figure 1a can indicate only that the pH of the solution was lowered to at least pH 3.0 after 90 min of operation. A similar experiment using quinaldine red as the pH indicator (pH $\leq$1.4, colorless; pH $\geq$3.2, red) showed that after spraying for about 95 min the solution at the tip of the platinum capillary had a pH $\leq$1.4 (Figure 1b). It is important to emphasize that the color indicative of this low pH is noted only at the wire tip. This downstream end of the wire electrode is where the current density and interfacial potential might be expected to be greatest. Thus, the greater amount of water electrolysis and corresponding pH drop take place at this point [9, 21].

A series of individual experiments like those illustrated in Figure 1 were performed with a stainless steel or platinum wire electrode and different indicator solutions to determine the pH at the wire tip as a function of spraying time. Care was taken to maintain very similar flow rates and ES currents in all the experiments. Clear trends were observed. The electrochemical oxidation of H_2O dropped the pH at the wire tip in the capillary in a roughly linear fashion with spraying time.

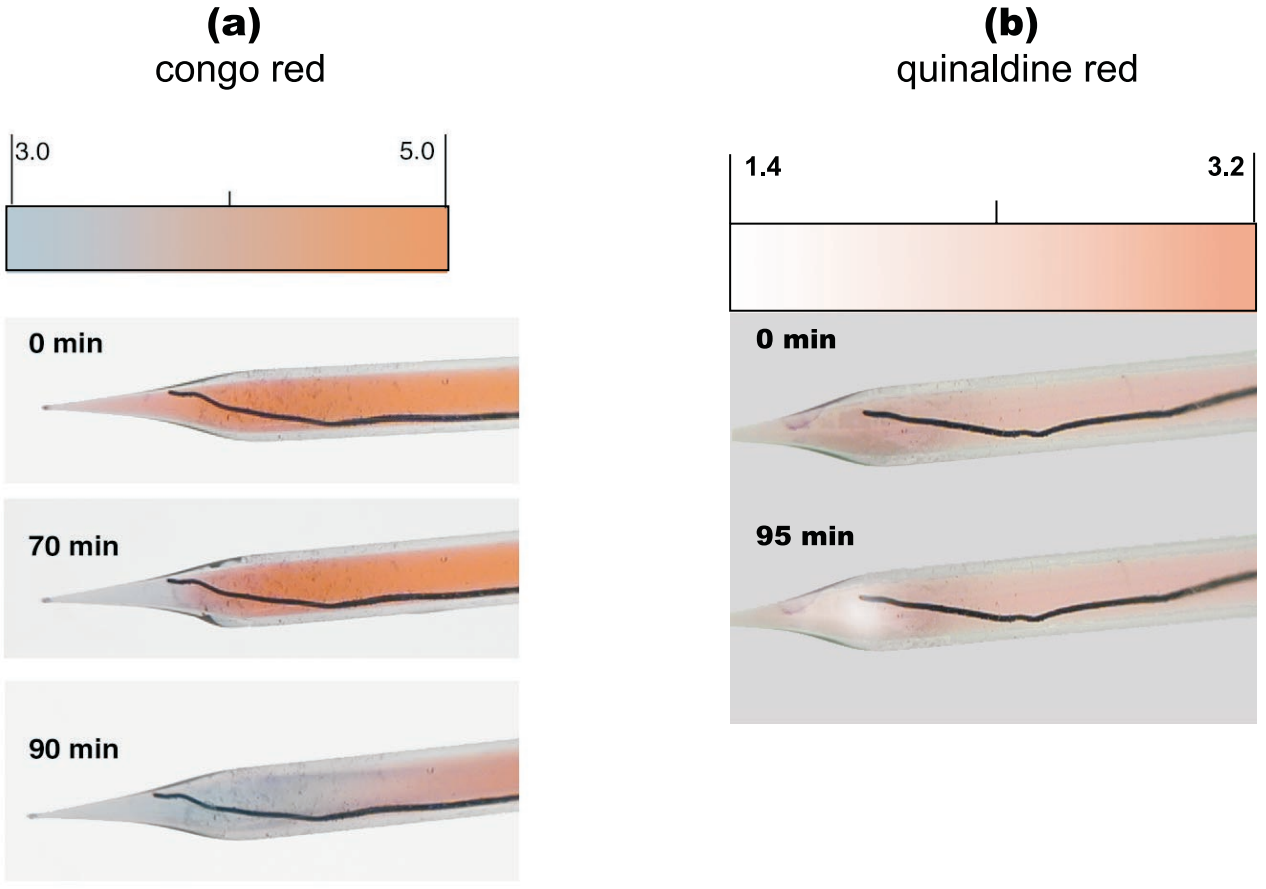

Figure 1. Time-lapsed photographs acquired at the indicated time intervals after application of 900 V to the platinum wire within a nano-ES capillary emitter containing a pH indicator. (**a**) Congo red photos obtained at 0 min, 70 min and 90 min. Initial solution composition: 0.1 wt% indicator in 85/15 (v/v) H_2O/CH_3OH, 0.1 mM KNO_3, pH ≈5.5. (**b**) Quinaldine red photos obtained at 0 min and 95 min. Initial solution composition: 0.1 wt% indicator in 85/15 (v/v) H_2O/CH_3OH, 0.1 mM KNO_3, pH ≈5.8.

The greatest magnitude of change in pH at any particular spray time occurred when the platinum electrode was used in an unbuffered solution. The magnitude of the pH change with a platinum electrode was mitigated when the solution sprayed contained 10 mM NH_4OAc as a pH buffer. Although our data was limited, the use of a stainless steel wire electrode generally had even more effect on minimizing the pH change than did the pH buffer. Corrosion of the stainless steel electrode, which would decrease the current efficiency for the oxidation of water, might explain this observation [18].

In summary, the combination of a pH buffer and the stainless steel (or another corrodible electrode), along with a short spraying time, might be the best combination to limit the extent of the pH change of the bulk solution in the capillary caused by the electrolytic reactions. On the other hand, use of a platinum or other inert wire electrode, an unbuffered solution, and a long spray time leads to the largest change in solution pH.

Conventional wisdom states that the gas-phase abundances of the ions in an ES mass spectrum reflect, at least qualitatively, the abundances of these ions present in solution. There are, of course, notable exceptions to this rule and the reasons for these discrepancies are of much fundamental interest [22, 23]. For analytes in which the equilibrium distribution of ions in solution is a function of pH (compounds with acidic or basic sites), or in situations where solution interactions that are to be preserved into the gas-phase are a function of solution pH (e.g., noncovalent interactions [24]), the electrochemically-induced pH change in a nano-ES capillary could be expected to significantly affect the ions and/or ion abundances in a spectrum. Thus, one should be cautious of the electrochemical alteration of solution

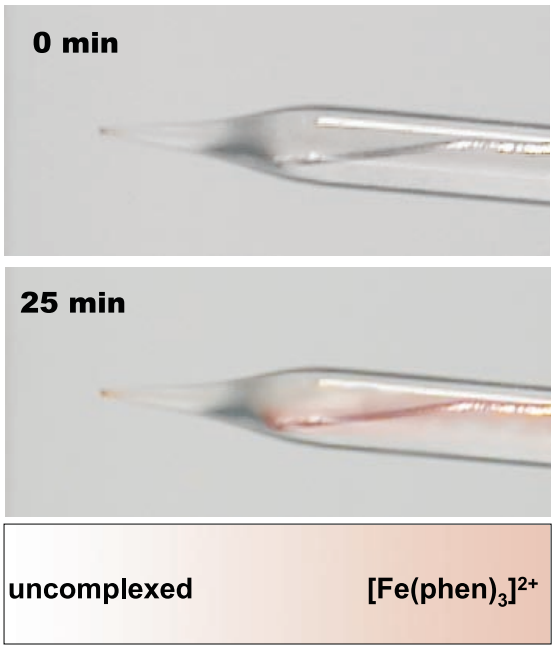

Figure 2. Time-lapsed photographs of the nano-ES capillary containing the iron (II) indicator, 1,10-phenanthroline (1.0 mM) in CH_3CN that were acquired 0 min and 25 min after application of 900 V to the iron wire electrode within the capillary solution.

pH in lengthy experiments with a nano-ES emitter of the wire-in-a-capillary design.

Anodic Corrosion of the High Voltage Contact to Solution

In positive ion mode, anodic corrosion (oxidation) of the metal electrode that makes electrical contact to solution may take place [14, 16, 25]. The extent of this reaction will be dependent largely on the redox characteristics of the metal, but it will also be influenced by current density and the nature of the solvent system. For example, corrosion of many metals is enhanced in acidic or chloride containing media [26].

Figure 2 shows the time lapse photographs of a nano-ES capillary before and during the spraying of an CH_3CN solution of 1.0 mM 1,10-phenanthroline using an iron wire as the high voltage contact to solution. It was expected that the iron wire would anodically corrode producing as the major product iron(II) (eq 4)

$$Fe^{2+} + 2e^- = Fe,\ E^o = -0.44V \text{ vs SHE [19]} \qquad (4)$$

Iron(II) forms the distinctive red $[Fe(phen)_3]^{2+}$ complex [27], which after 25 min of continuous spraying, can be observed in the photograph in Figure 2. The expected red color of the complex is seen to surround the wire along its total length in the photo. This indicates that the corrosion process not only occurs at the tip of the wire nearest to the spray, but also a substantial distance upstream into the capillary. While the interfacial electrode potential is known to fall off rapidly upstream along the electrode in an ES emitter [21], these results indicate that the potential necessary for iron corrosion extends a considerable distance upstream of the wire tip. Visual inspection of the iron wire after use showed what appeared to be rust along the length of the wire that had been immersed in the solution within the capillary. Thus, while the oxidation of water at the platinum wire occurred mainly at the tip of the wire, the electrochemically more facile corrosion of an iron wire occurred a substantial distance along its length upstream into the capillary.

The photographs in Figure 2 can only be used to confirm the presence of the iron(II) as a corrosion product. However, phenanthroline complexes of a number of other cations that cannot be detected by visible solution color changes do form [27]. Some of these metal ions as phenanthroline complexes can be detected in the gas-phase. To illustrate, the ES mass spectra recorded when spraying an CH_3CN/1.0 mM 1,10-phenanthroline solution from a pulled-glass nano-ES emitter with platinum, stainless steel, iron, and copper wire electrodes are shown in Figure 3. When using the platinum wire electrode (Figure 3a), the two major ions observed in the spectrum were those corresponding to the protonated and sodiated phenanthroline at *m/z* 181 and 203, respectively. The origin of some of the protons might be traces of acid in the solvent or oxidation of water in the solvent at the tip of the platinum wire. A major source of the Na^+ cations might be the glass of the capillary. Corrosion of the platinum was not expected nor was any evidence of its occurrence noted by the nature of the ions observed in the spectra. When a stainless steel electrode was used (Figure 3b), ions were again observed for the protonated (*m/z* 181) and sodiated (*m/z* 203 and 383) phenanthroline. Also, ions attributed to a double-charge iron(II) phenanthroline complex, $[Fe(phen)_2)]^{2+}$ (*m/z* 208), were observed. Single-charge copper(I), $[Cu(phen)_2)]^+$ (*m/z* 423), and double-charge copper(II), $[Cu(phen)_2)]^{2+}$ (*m/z* 211.5) phenanthroline complexes, were observed in the spectrum. The presence of the complexes of iron(II), copper(I), and copper(II) in the spectrum indicates that the stainless steel wire was corroding and that the stainless steel wire contained a substantial amount of copper. When using the same iron wire as shown in the photo in Figure 2 as the electrode, the major ions observed still included the protonated and sodiated forms of phenanthroline (*m/z* 181, 203 and 383) (Figure 3c). However, the relative abundances of the iron(II), copper(I), and copper(II) phen complexes increased indicating a greater extent of corrosion. This wire was salvaged from a J-type thermocouple and the purity was unknown. However, the peaks observed in this spectrum indicate it must contain a substantial amount of copper. In this spectrum, the peak at *m/z* 298 attributed to $[Fe(phen)_3]^{2+}$ was clearly visible above the background. This peak was not as abundant when

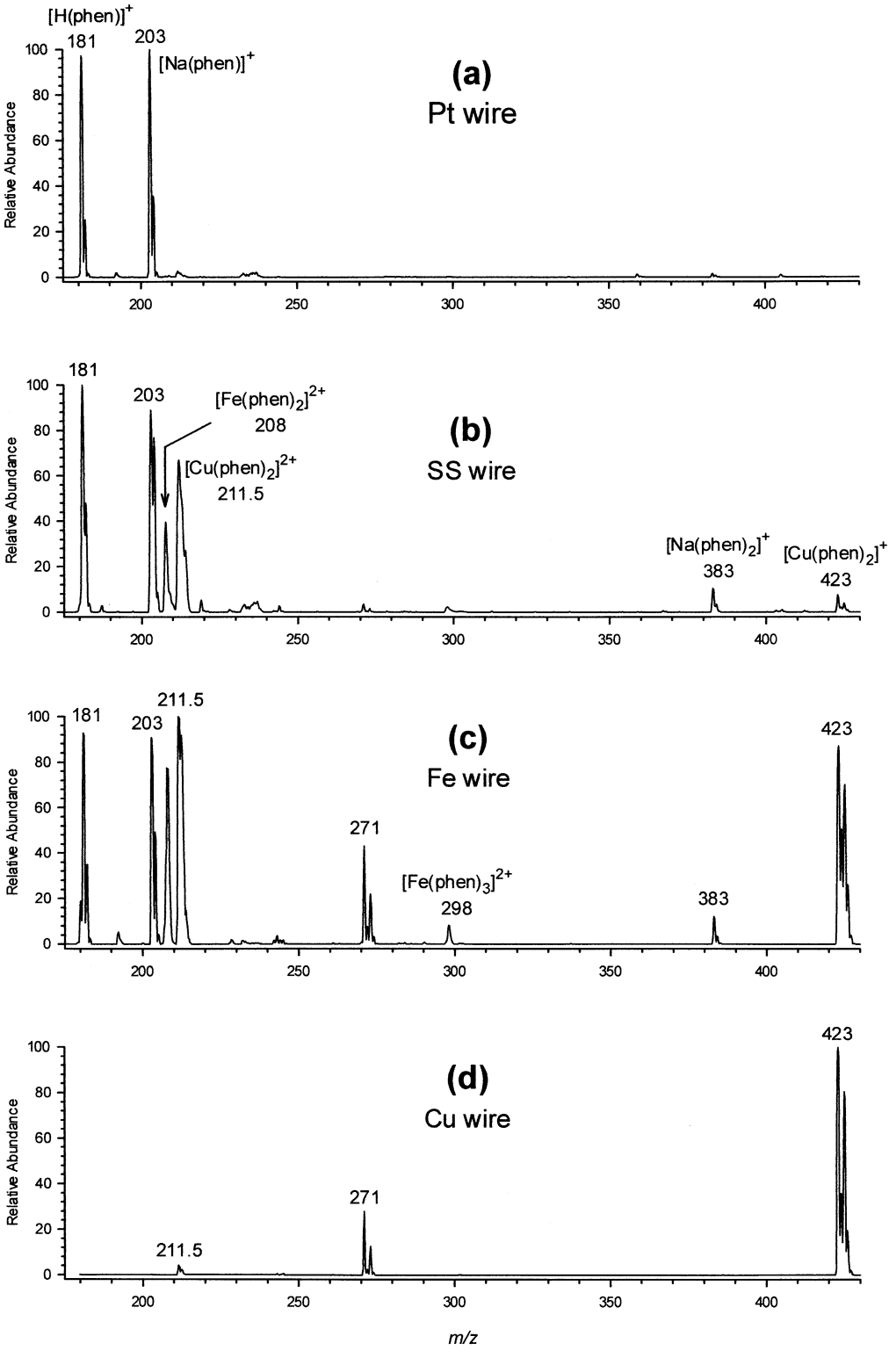

Figure 3. Average ES mass spectra recorded from approximately 20–25 min into the analyses when spraying CH_3CN containing 1,10-phenanthroline (1.0 mM) from a nano-ES emitter using a (**a**) platinum, (**b**) stainless steel, (**c**) iron, or (**d**) copper wire electrode contact to solution.

using the harder-to-oxidize stainless steel wire electrode. Also, a new but unidentified single-charge copper complex was observed at *m/z* 271.

Because the stainless steel and iron wires contained a substantial amount of copper, we decided to investigate the use of a pure copper wire electrode. The resulting spectrum, shown in Figure 3d, was simpler than that obtained using either a stainless steel or iron wire. No

protonated or sodiated phenanthroline ions were observed. Apparently enough copper was introduced into the system to bind all the phenanthroline present. The copper(I) complex, $[Cu(phen)_2]^+$, at *m/z* 423, was the base peak in the spectrum, while the unidentified complex at *m/z* 271 was present at about 30% relative abundance. The copper(II) complex, $[Cu(phen)_2]^{2+}$ at *m/z* 211.5, that was a dominate peak in the spectra in Figures 3b and 3c, was observed at only about 5% relative abundance.

The data in Figure 3 demonstrate that the metal wire used to make electrical contact in the ES capillary may corrode. The particular alloy or pure metal electrode and the solvent/ligand system appear to control the redox state and abundance of some of the metal ions observed in the gas-phase [e.g., copper(I) versus copper (II)]. In the presence of one another, the various solvents and ligands, and the metallic electrode, the various metal ions liberated into solution electrochemically might be expected to undergo a variety of heterogenous and/or homogenous redox reactions that influence the ultimate distribution of the metal species sprayed from the capillary [26, 28]. These same data also illustrate that electrode corrosion might be used to supply metal ions to solution for the study of metal-ligand complex chemistry (e.g., [29, 30]), or to ionize particular molecules by metal-analyte cationization (e.g., [30–33]). This approach to adding metal ions to solution might therefore be a complementary or an alternative approach to adding the metal salts to solution prior to analysis [29–33]. This could be particularly useful when the salts are relatively insoluble or the metal ions are only short-lived (e.g., copper (I) in water [28]) in the solvent in which they are prepared.

Analyte Oxidation at the High Voltage Contact

The analyte of interest may also be involved in the electrochemical reactions at the electrical contact to solution. Depending on the analysis scenario, this can be good or bad [16]. Involvement of the analyte in the electrochemical process may be bad, for example, if the analyte is an unknown and the mass or charge state is altered. This might result in an incorrect mass or speciation determination. Involvement of the analyte in the electrochemical process might be deemed good if, as is shown below, a neutral analyte not normally detected by ES-MS is ionized electrochemically. In this way, the molecule becomes detectable.

Experiments with a conventional ES ion source incorporating either a stainless steel or platinum capillary emitter electrode have demonstrated that nickel(II) octaethylporphyrin (NiOEP) can be ionized electrochemically inside the capillary and the ions so formed can be efficiently detected in the gas-phase [34, 35]. NiOEP is a neutral molecule that is oxidized by consecutive electron-transfer forming first the molecular radical cation, $M^{+\bullet}$ (E_{peak1} = 1.08 V vs SHE), and then the dication, M^{2+} (E_{peak2} = 1.61 V vs SHE) [36]. Formation of the dication in the previous ES-MS experiments required the use of a platinum capillary emitter, high electrolyte concentrations (1.0 mM lithium triflate) and a slow solution flow rate ($\leq$2.5 μL/min).

The data in Figure 4 illustrate the observations made when this same porphyrin was sprayed from a nano-ES emitter using a platinum wire electrode. The high voltage was applied to the wire about 30 s after the mass spectrometer started to record data. When the high voltage was switched on, the total ion current (TIC) rapidly reached a maximum value (Figure 4a). The TIC fell gradually to about 50% of the original value after 7 min, and then rose gradually up to 75% over the remaining 23 min of the experiment. The extracted ion current profile for the molecular ions (*m/z* 590) of the porphyrin is shown in Figure 4b. For the first 7 min of the experiment, no ions owing to the porphyrin were observed in the spectrum. This is further illustrated by the mass spectrum of the molecular ion region obtained at 5 min (Figure 4c), which is devoid of any peaks. At about 7.5 min, the porphyrin molecular ions are first observed (Figure 4b). The abundance of these ions continued to increase over a period of 7 min reaching a plateau at about 15 min, but even at this point they contribute only a small fraction of the TIC. The majority of the ion current at all times was due to ions at *m/z* 350. The spectrum recorded at 15 min (Figure 4d) contains the isotopic cluster of the molecular species spanning *m/z* 590–594. Note that there was no sign of the dication at *m/z* 295 (this area of spectrum not shown) at this time or elsewhere during the course of the experiment.

When using the wire-in-a-capillary arrangement for the high voltage contact to solution, the delayed observance of the porphyrin radical cations was always the case. However, variations in the wire placement from experiment to experiment affected the length of the time delay. Such delay periods are to be expected in all ES emitters in which the high voltage contact to solution is made upstream of the emitter spray tip [34, 37]. The products of the electrochemical reactions formed at the point of the electrode contact to solution must be transported to the spray tip, which can cause a significant time delay between their formation in solution and their detection in the gas-phase.

As the time of analysis continued beyond 15 min in this experiment, new single-charge peak clusters appeared at *m/z* values greater than that of the porphyrin molecular ion. This can be seen by comparing the spectra acquired at 15 min (Figure 4d) and 25 min (Figure 4e). From the masses and isotope cluster patterns, these new ions must be the result of the addition of one and two chlorine atoms into the porphyrin macrocycle, viz., $(M - H + Cl)^+$ and $(M - 2H + 2Cl)^+$, respectively. Two lesser abundant peak clusters at higher *m/z* (not shown) were also observed. These corresponded to products containing three and four chlorine atoms, respectively.

Two possible pathways of formation of the chlorinated products may be postulated. The first involves

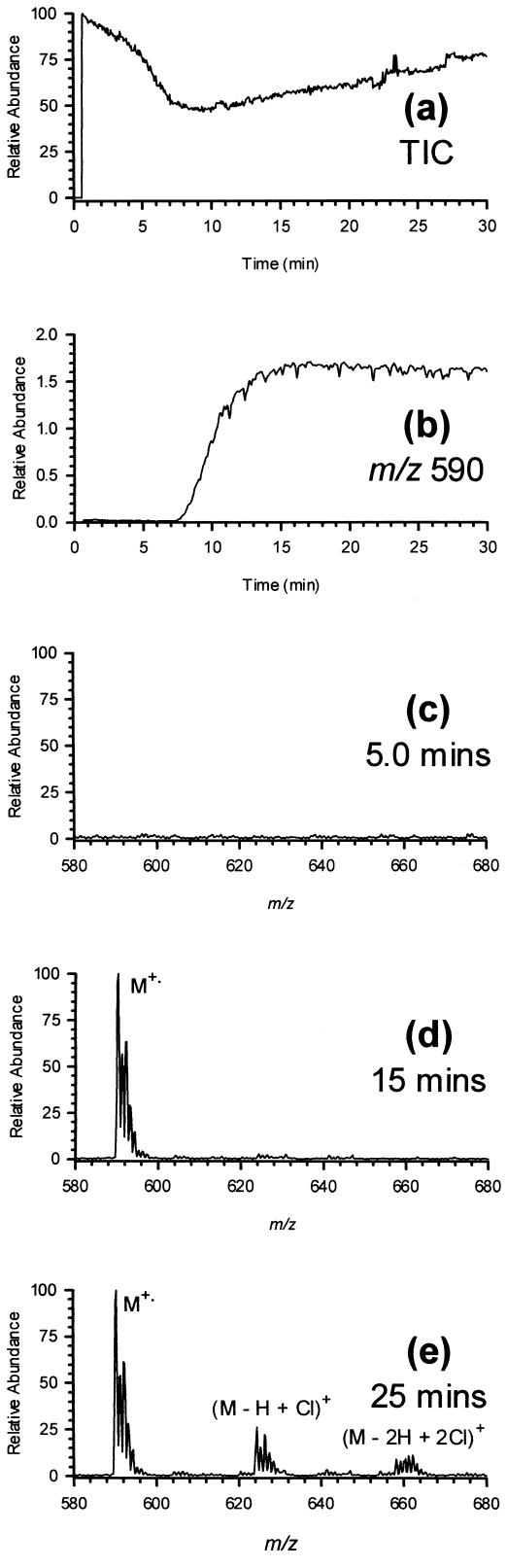

Figure 4. Plots showing (**a**) total ion current and (**b**) extracted ion current profiles for the radical cation of NiOEP (*m/z* 590) recorded when spraying an 8.4 μM NiOEP solution (CH_2Cl_2/CH_3CN (1/1 v/v), 1.0 mM lithium triflate) from a nano-ES emitter with the 900 V electrical contact to solution made via a platinum wire electrode. The molecular ion region of the mass spectrum recorded at (**c**) 5.0 min, (**d**) 15 min, and (**e**) 25 min into the analysis is also shown.

reaction of the radical cation, or the more reactive dication (this is possibly the reason why it is not observed), with chloride ion present as an impurity in the solvents. The grade of CH_2Cl_2 used in these experiments, for example, may contain up to 10 ppm Cl^-. Sequential reaction and reoxidation of the chlorinated intermediates would lead to the multiple additions of Cl observed. Such a chlorination scheme has been proposed for the radical cation of 9,10-diphenylanthracene [38]. A second possibility is that the CH_2Cl_2 is oxidized at the platinum wire electrode forming radicals and/or molecular chlorine [39] that subsequently reacts with the porphyrin. In either case, the observation of these chemical followup reaction products is related to the long delay period between initial oxidation of the analyte and the transfer to the gas-phase owing to the upstream electrode configuration. Such products were not observed when spraying from a platinum capillary at flow rates as low as 1.5 μL/min [35].

The data in Figure 4 provides a strong example that the nature of the nano-ES mass spectrum, when using the wire-in-a-capillary electrode geometry, can be quite dependent on the time period during the analysis in which the spectrum is recorded. The temporal changes in the spectra noted here were a direct result of the ongoing electrochemical and chemical reactions upstream in the emitter capillary.

Conclusions

Electrochemical reactions occur at the electrode contact to solution in the ES emitter of all ES ion sources. The results presented here show that the wire-in-a-capillary electrode geometry, bulk-loaded nano-ES emitter is no different. These data illustrate electrochemical reactions of three major types, viz., solvent oxidation (i.e., H_2O oxidation), emitter electrode corrosion (stainless steel, iron, and copper wire corrosion), and analyte oxidation (NiOEP oxidation). The products of each of the three reaction types alter the composition of the initial solution placed in the nano-ES emitter capillary. Depending on the particular analysis scenario (solvent, ES currents, flow rates, electrode material, etc.) and on the analyte chemical properties (pK_a, metal-binding affinity, equilibrium redox potential, etc.), these alterations of solution composition (pH, metal ion concentration, analyte charge state, etc.) might affect the appearance of the mass spectra acquired.

As a whole, these data demonstrate that the solution composition and the nature of the nano-ES mass spectrum, when using the wire-in-a-capillary electrode geometry, can be quite time dependent. These changes in the spectrum with time can be a result of the ongoing electrochemical and possibly also chemical reactions upstream in the emitter capillary. Like all other ES emitters in which the electrical contact to solution is made upstream of the emitter spray tip, there can be a significant delay time between the formation of electrolysis products at the emitter electrode and the gas-phase

detection of the products. Unlike a pumped ES device, or probably a metal-coated glass nano-ES capillary, the products of the electrochemical reactions formed in a bulk-loaded, wire-in-a-capillary nano-ES emitter are not necessarily swept directly from the capillary out into the spray. The whole volume of solution within the capillary can be altered because of mass transport (e.g., diffusion) of the products formed at the spray tip end of the wire throughout the volume. This means that the magnitude of alteration in solution composition caused by the electrochemical reactions may not be simply calculated from the ES current and solution flow rate using Faraday's law. Also, the choice of the wire electrode material will in some cases have a substantial influence on what electrochemical reactions occur and on what ions are observed in the gas-phase.

Acknowledgments

P.D.S. acknowledges support through an appointment to the Oak Ridge National Laboratory (ORNL) Postdoctoral Research Associates Program administered jointly by the Oak Ridge Institute for Science and Education and ORNL. ES-MS instrumentation was provided in part by a Cooperative Research and Development Agreement with MDS SCIEX (CRADA No. ORNL96-0458). This research was sponsored by the Division of Chemical Sciences, Geosciences, and Biosciences, Office of Basic Energy Sciences, United States Department of Energy, under Contract DE-AC05-00OR22725 with ORNL, managed and operated by UT-Battelle, LLC.

The submitted manuscript has been authorized by a contractor of the U.S. Government under contract no. DE-AC05-00OR22725. Accordingly, the U.S. Government retains a paid-up, nonexclusive, irrevocable, worldwide license to publish or reproduce the published form of this contribution, prepare derivative works, distribute copies to the public, and perform publicly and display publicly, or allow others to do so, for U.S. Government purposes.

References

1. Karas, M.; Bahr, U.; Dülcks, T. Nano-Electrospray Ionization Mass Spectrometry; Addressing Analytical Problems Beyond Routine. *Fresnius J. Anal. Chem.* **2000,** *366*, 669–676.
2. Wilm, M. S.; Mann, M. Electrospray and Taylor-Cone Theory, Dole's Beam of Macromolecules at Last? *Int. J. Mass Spectrom. Ion Processes* **1994,** *136*, 167–180.
3. Wilm, M. S.; Mann, M. Analytical Properties of the Nanoelectrospray Ion Source. *Anal. Chem.* **1996,** *68*, 1–8.
4. Kirby, D. P.; Thorne, J. M.; Götzinger, W. K.; Karger, B. L. A CE/ESI-MS interface for Stable, Low Flow Operation. *Anal. Chem.* **1996,** *68*, 4451–4457.
5. Cao, P.; Moini, M. A Novel Sheathless Interface for Capillary Electrophoresis/Electrospray Ionization Mass Spectrometry Using an In-capillary Electrode. *J. Am. Soc. Mass Spectrom.* **1997,** *8*, 561–564.
6. Oosterkamp, A. J.; Gelpí, E.; Abian, J. Quantitative Peptide Bioanalysis Using Column-switching Nano Liquid Chromatography/Mass Spectrometry. *J. Mass Spectrom.* **1998,** *33*, 976–983.
7. Geromanos, S.; Philip, J.; Freckleton, G.; Tempst, P. In*J*ectable *a*daptable *F*ine *I*onization *S*ource (JaFIS) for Continuous Flow Nano-electrospray. *Rapid Commun. Mass Spectrom.* **1998,** *12*, 551–556.
8. Maziarz, E. P.; Lorenz, S.A.; White, T. P; Wood, T. D. Polyaniline: A Conductive Polymer Coating for Durable Nanospray Emitters. *J. Am. Soc. Mass Spectrom.* **2000,** *11*, 659–663.
9. Van Berkel, G. J. Insights into Analyte Electrolysis in an Electrospray Emitter from Chronopotentiometry Experiments and Mass Transport Calculations. *J. Am. Soc. Mass Spectrom.* **2000,** *11*, 951–960.
10. Kriger, M. S.; Cook, K. D.; Ramsey, R. S. Durable Gold-Coated Fused Silica Capillaries for Use in Electrospray Mass Spectrometry. *Anal. Chem.* **1995,** *67*, 385–389.
11. Valaskovic, G. A.; McLafferty, F. W. Long-Lived Metallized Tips for Nanoliter Electrospray Mass Spectrometry. *J. Am. Soc. Mass Spectrom.* **1996,** *7*, 1270–1272.
12. Andrien, B. A.; Sauro, D. M.; Sansone, M. A.; Whitehouse, G. P.; Whitehouse, C. M.; Burt, A. G. A Disposable μ-Tip Probe for Low Flow Electrospray. *Proceedings of the 45th ASMS Conference on Mass Spectrometry and Allied Topics*; Palm Springs, CA, June, 1997; p 457.
13. Fong, K. W. Y.; Chan, T.-W. D. A Novel Nonmetallized Tip for Electrospray Mass Spectrometry at Nanoliter Flow Rate. *J. Am. Soc. Mass Spectrom.* **1999,** *10*, 72–75.
14. Blades, A. T.; Ikonomou, M. G.; Kebarle, P. Mechanism of Electrospray Mass Spectrometry. Electrospray as an Electrolysis Cell. *Anal. Chem.* **1991,** *63*, 2109–2114.
15. Van Berkel, G. J.; Zhou, F. Characterization of an Electrospray Ion Source as a Controlled-Current Electrolytic Cell. *Anal. Chem.* **1999,** *64*, 1586–1593.
16. Van Berkel, G. J. The Electrolytic Nature of Electrospray. In *Electrospray Ionization Mass Spectrometry*; Cole, R. B., Ed., Wiley: New York, 1997; Chap I, pp 65–105.
17. Green, F. J. *The Sigma-Aldrich Handbook of Stains, Dyes and Indicators*; Aldrich Chemical Company: Milwaukee, WI, 1990.
18. Van Berkel, G. J.; Zhou, F.; Aronson, J. T. Changes in Bulk Solution pH Caused by the Inherent Controlled-Current Electrolytic Process of an Electrospray Ion Source. *Int. J. Mass Spectrom. Ion Processes* **1997,** *162*, 55–67.
19. Dobos, D. *Electrochemical Data*; Elsevier: Amsterdam, 1975.
20. Kebarle, P.; Tang, L. From Ions in Solution to Ions in the Gas Phase. The Mechanism of Electrospray Mass Spectrometry. *Anal. Chem.* **1993,** *65*, 972A–986A.
21. Van Berkel, G. J.; Giles, G. E.; Bullock, J. S., IV; Gray L. J. Novel Computational Simulation of Redox Reactions within a Metal Electrospray Emitter. *Anal. Chem.* **1999,** *71*, 5288–5296.
22. Mansoori, B. A.; Volmer, D. A.; Boyd, R. K. Wrong-Way Round Electrospray Ionization of Amino Acids. *Rapid Commun. Mass Spectrom.* **1997,** *11*, 1120–1130.
23. Zhou. S.; Cook, K. D. Protonation in Electrospray Mass Spectrometry: Wrong-Way-Round or Right-Way-Round. *J. Am. Soc. Mass Spectrom.* **2000,** *11*, 961–966.
24. Jorgensen, T. J. D.; Roepstorff, P.; Heck, A. J. R. Direct Determination of Solution Binding Constants for Noncovalent Complexes between Bacterial Cell Wall Peptide Analogues and Vancomycin Group Antibiotics by Electrospray Ionization Mass Spectrometry. *Anal. Chem.* **1998,** *70*, 4427–4432.
25. Van Berkel, G. J. Electrolytic Corrosion of a Stainless-Steel Electrospray Emitter Monitored using an Electrospray-Photodiode Array System. *J. Anal. At. Spectrom.* **1998,** *13*, 603–607.
26. Sawyer, D. T.; Sobkowiak, A.; Roberts, J. L., Jr. *Electrochemistry for Chemists*; Wiley: New York, 1995.
27. Marczenko, Z. *Spectrophotometric Determination of Elements*; Halsted Press: New York, 1976.
28. Cotton, F. A.; Wilkinson, G. *Advance Inorganic Chemistry*; Wiley: New York, 1980.
29. Li, H.; Siu, K. W. M.; Gueremont, R.; Le Blanc, J. C. Y. Complexes of Silver(I) with Peptides and Proteins as Produced by Electrospray Mass Spectrometry. *J. Am. Soc. Mass Spectrom.* **1997,** *8*, 781–792.
30. Gatlin, C. L.; Tureček, F. Quantitative Electrospray Ionization

Mass Spectrometric Studies of Ternary Complexes of Amino Acids with Cu^{2+} and Phenanthroline. *J. Mass Spectrom.* **2000,** *35*, 172–177.
31. Alverez, E. J.; Brodbelt, J. S. Evaluation of Metal Complexation as an Alternative to Protonation for Electrospray Ionization of Pharmaceutical Compounds. *J. Am. Soc. Mass Spectrom.* **1998,** *9*, 463–472.
32. Rentel, C.; Strohschein, S.; Albert, K.; Bayer, E. Silver-Plated Vitamins: A Method of Detecting Tocopherols and Carotenoids in LC/ESI-MS Coupling. *Anal. Chem.* **1998,** *70,* 4394–4400.
33. Bayer, E.; Gfrörer, P.; Rentel, C. Coordination-Ionspray-MS (CIS-MS), a Universal Detection and Characterization Method for Direct Coupling with Separation Techniques. *Angew. Chem. Int. Ed.* **1999,** *38*, 992–995.
34. Van Berkel, G. J.; McLuckey, S. A.; Glish, G. L. Electrochemical Origin of Radical Cations Observed in Electrospray Ionization Mass Spectra. *Anal. Chem.* **1992,** *64,* 1586–1593.
35. Van Berkel, G. J; Zhou, F. Observation of Gas-Phase Molecular Dications Formed from Neutral Organics in Solution via the Controlled-Current Electrolytic Process Inherent to Electrospray. *J. Am. Soc. Mass Spectrom.* **1996,** *7*, 157–162.
36. Van Berkel, G. J.; Zhou, F. Chemical Electron-Transfer Reactions in Electrospray Mass Spectrometry: Effective Oxidation Potentials of Electron Transfer Reagents in Methylene Chloride. *Anal. Chem.* **1994,** *66*, 3408–3415.
37. Van Berkel, G. J. Electrolytic Deposition of Metals on to the High-Voltage Contact in an Electrospray Emitter: Implications for Gas-Phase Ion Formation. *J. Mass Spectrom.* **2000,** *35*, 773–783.
38. Yoshida, K. *Electrooxidation in Organic Chemistry*; Wiley: New York, 1984.
39. Mann, C. K. Nonaqueous Solvents for Electrochemical Use. In *Electroanalytical Chemistry, Vol. III*; Bard, A. J., Ed.; Marcel Dekker: New York, 1969; pp. 57–134.